01 Jul 2005

Calculation of Hydrogenic Bethe Logarithms for Rydberg States

Ulrich D. Jentschura
Missouri University of Science and Technology, ulj@mst.edu

Peter J. Mohr

Recommended Citation

U. D. Jentschura and P. J. Mohr, "Calculation of Hydrogenic Bethe Logarithms for Rydberg States," *Physical Review A - Atomic, Molecular, and Optical Physics*, vol. 72, no. 1, pp. 012110-1-012110-9, American Physical Society (APS), Jul 2005.
The definitive version is available at https://doi.org/10.1103/PhysRevA.72.012110

Calculation of hydrogenic Bethe logarithms for Rydberg states

Ulrich D. Jentschura[1,2] and Peter J. Mohr[2]
[1]*Max-Planck-Institut für Kernphysik, Saupfercheckweg 1, 69117 Heidelberg, Germany*
[2]*National Institute of Standards and Technology, Gaithersburg, Maryland 20899-8401, USA*
(Received 1 April 2005; published 19 July 2005)

We describe the calculation of hydrogenic (one-loop) Bethe logarithms for all states with principal quantum numbers $n \leqslant 200$. While, in principle, the calculation of the Bethe logarithm is a rather easy computational problem involving only the nonrelativistic (Schrödinger) theory of the hydrogen atom, certain calculational difficulties affect highly excited states, and in particular states for which the principal quantum number is much larger than the orbital angular momentum quantum number. Two evaluation methods are contrasted. One of these is based on the calculation of the principal value of a specific integral over a virtual photon energy. The other method relies directly on the spectral representation of the Schrödinger–Coulomb propagator. Selected numerical results are presented. The full set of values is available at arXiv.org/quant-ph/0504002.

DOI: 10.1103/PhysRevA.72.012110 PACS number(s): 12.20.Ds, 31.30.Jv, 06.20.Jr, 31.15.−p

I. INTRODUCTION

The evaluation of the Bethe logarithm, in 1947 [1], was carried out using one of the first automatized devices for the implementation of numerical calculations in physics. Today, the evaluation of the (one-loop) Bethe logarithm for the ground state of hydrogen to about ten figures of accuracy can be carried in less than a second on a modern workstation. Consequently, one might be tempted ask why there should be yet another paper on Bethe logarithms in the first place? The answer is threefold: (i) In the context of recent efforts toward an improved understanding of the hydrogen and deuterium spectra [2] (see also physics.nist.gov/hdel), we have strived to increase the number of states for which this basic quantum electrodynamic correction is known. (ii) The Bethe logarithm has been found to follow a characteristic asymptotic structure, expressible in terms of a series in inverse powers of the principal quantum numbers. This asymptotic structure has been found to be applicable to wide classes of quantum electrodynamic effects in atoms [3–5]. Consequently, it appeared to be of interest to verify these asymptotic properties by explicit calculations of the Bethe logarithm for very highly excited states. (iii) The most comprehensive collection of Bethe logarithms recorded so far in the literature [6] extends up to the principal quantum number $n=20$. Here, we consider levels up to $n=200$. This should be contrasted with recent experimental investigations [7] that were carried out with states of principal quantum numbers as high as $n=30$.

Frequency combs can lead to tremendous simplifications for high-precision spectroscopic experiments (e.g. Ref. [8–15]). In the future, it should become feasible to carry out high-precision experiments on transitions much more effectively than in the past. Rydberg states with long natural lifetimes are rather promising candidates for precision metrology, and one might imagine either direct transitions among Rydberg states or optical transitions from, e.g., the metastable $2S$ state to a highly excited D state. Such measurements might contribute to future advances in our knowledge of the hydrogen and deuterium spectra. On the theoretical side, the method of least squares [2] allows for a self-consistent adjustment of fundamental constants, such as the Rydberg constant and the proton charge radius, using experimental input data from more than one transition. The investigation reported here is an element of a project (see also Ref. [2]) to enlarge the 2002 adjustment of constants [16] so as to provide optimal predictions for energy levels not contained in this adjustment, consistent with the values of the constants used in that adjustment.

Thus, we here discuss the evaluation of Bethe logarithms using two different methods:

(i) An integral representation which is based on analytic calculations using the Sturmian representation of the Schrödinger–Coulomb Green function, and

(ii) A spectral representation which relies on known results for the transition matrix elements of discrete-discrete and discrete-continuum transitions of hydrogen.

The two methods are found to be suitable for different ranges of principal and angular momentum quantum numbers. While a complete account of all previous work on the Bethe logarithm would result in an excessively long list of references, it might be instructive and appropriate to recall a few previous investigations on this subject [17–27]. Recently, the Bethe logarithm was re-evaluated, for selected hydrogenic states, in the context of lower-order terms acting as preparatory calculations for higher-order relativistic corrections to the self-energy [28–30]. The basic equation defining the spectral decomposition has been given in Eq. (2a) of Ref [25] and the basic equation for the integral representation has been indicated in Eq. (2b) of Ref. [25]. The evaluation for low-lying states of hydrogen, using the two methods, has previously been discussed in Secs. IIB (integral representation) and IIC (spectral representation) of the comprehensive Ref. [25]. A similar, though less comprehensive, comparison of the two approaches had been made previously in Ref. [22]. In the context of the spectral representation, we recall that in Table II of Ref. [17] and Table I of Ref. [18], one may even find results for the particular contributions of the discrete spectrum and of the continuum to the Bethe logarithm of selected low-lying states. In general, we found that unexpected numerical difficulties affect the calculation of Bethe logarithms for Rydberg states, especially in cases where the difference $n-l$ of the principal quantum number n

and the orbital quantum number l is large. Here, we attempt to enhance both the range of applicability of the integral representation as well as the spectral representation, by the use of convergence acceleration methods [31,32] for the evaluation of hypergeometric functions that characterize propagator matrix elements (integral representation) and the calculation of infinite sums over discrete virtual intermediate states (spectral representation).

(At least) two further methods are available for the evaluation of Bethe logarithms: One of these is based on the determination of approximate eigenfunctions obtained using finite basis sets [24], which may be combined with a Neville–Richardson extrapolation to yield accurate values, thereby decreasing the required number of functions in the basis set. Basis-set methods are also used in calculations of Bethe logarithms in helium (see e.g., Ref. [33,34]). A fourth method relies on a discrete-space (lattice) evaluation of the radial component of the Schrödinger–Coulomb propagator [35,36]. This method is briefly discussed in Appendix A.

A somewhat special role is played by circular Rydberg states with $n-1=l=|m|$ [5], whose probability density around the atomic nucleus approximately has the shape of a rotationally symmetric, "circular" tire (see Fig. 1 of Ref. [5]), but this shape is restricted to the highest possible magnetic angular momentum projection. Because the Bethe logarithm does not depend on m, we will refer to all states with $n-l=1$ as circular states in this article. Circular states have the highest possible l for given n. In the context of the current numerical investigation, it thus appears useful to define a "noncircularity" or "angular-momentum defect" $\zeta=n-l\geqslant 1$. The radial hydrogenic wave functions have the structure of an exponential $\exp[-r/(na_0)]$, where a_0 is the Bohr radius, multiplied by a polynomial in r with ζ terms. The coefficients of this polynomial have an alternating sign pattern. Finite sums, whose terms display an alternating sign pattern, are notoriously problematic in numerical evaluations, because their convergence cannot be accelerated with the methods used for infinite series, and the straightforward summation of the terms, using multiprecision arithmetic, is often the only practical route to a reliable numerical evaluation.

This paper is organized as follows. In Sec. II, we discuss the integral representation of the Bethe logarithm and its application to the calculation of levels with small $n-l$. In Sec. III, we discuss the spectral representation. Some brief conclusions are drawn in Sec. IV.

II. INTEGRAL REPRESENTATION

As is customary for quantum electrodynamic bound-state calculations, we use a system of units in which $\hbar=c=\epsilon_0=1$. The Bethe logarithm is a low-energy second-order perturbation which is due to virtual states with one photon mode excited, and the atom in a virtual state. This can be seen most clearly by going to the Schrödinger-picture representation of the field operators [37]. A detailed discussion of the transition to the Schrödinger picture for the field operators, together with a basic application to bound-state problems, is given in Ref. [38]. The calculation naturally leads to an integral over the virtual photon energy which involves a hydrogenic Green function with an argument $z=E_n-\omega$, where ω is the energy of the virtual photon. In the literature, it is customary to set $z=-(Z\alpha)^2m/(2n^2t^2)$ (see, e.g., Ref. [28]). So t is a variable which parameterizes the argument of the Green function in terms of a generalized quantum number "$n\to nt$." Of course, the variable t has nothing to do with temporal evolution. Solving for t, we obtain

$$t=\frac{1}{\sqrt{1+\dfrac{2n^2\omega}{(Z\alpha)^2m}}}. \tag{1}$$

Here, m is the electron mass, Z is the nuclear charge, and α is the fine-structure constant. The photon energy can be expressed in terms of t as

$$\omega=\frac{1-t^2}{t^2}\frac{(Z\alpha)^2m}{2n^2}. \tag{2}$$

We denote the reference state by $|nlm\rangle$. The relevant matrix element, which involves the Schrödinger–Coulomb propagator, is given by

$$P_{nl}(t)=\frac{1}{3m}\left\langle nlm\left|p^i\frac{1}{H-E+\omega(t)}p^i\right|nlm\right\rangle, \tag{3}$$

where the summation convention is used for the sum over Cartesian coordinates ($i=1,2,3$). The integral representation for the Bethe logarithm $\ln k_0(n,l)$, in terms of $P(t)$, is different for S states ($l=0$) in comparison to non-S states ($l\neq 0$),

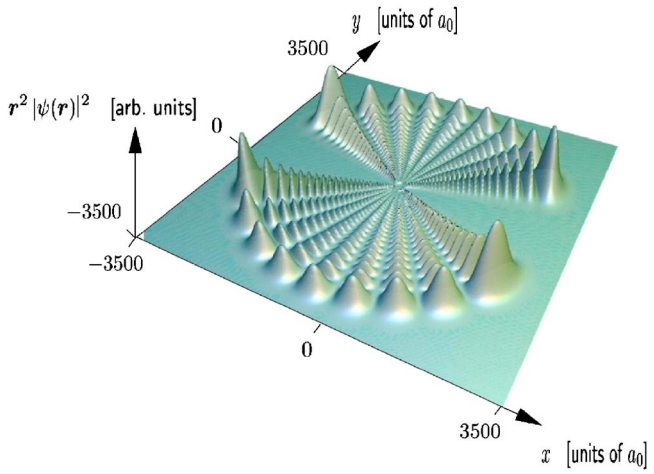

FIG. 1. (Color online.) The number of terms in the radial wave function grows with the principal quantum number n and with the angular momentum defect $\zeta=n-l$. In order to illustrate this well-known fact, we here plot the radial probability density of the state with quantum numbers $n=40, l=14$, and $m=6$, in the plane of constant azimuth $\phi=0$. Here, a_0 denotes the Bohr radius $a_0=\hbar/(\alpha mc)=0.529\,177\,2108(18)\times 10^{-10}$ m [16]. The Bethe logarithm for the state under discussion reads $\ln k_0(n=40,l=14)=-0.418,087,713\times 10^{-4}$.

$$\ln k_0(n,l) = -\frac{3}{4}(\mathrm{P}\,.\,\mathrm{V}\,.)\int_0^1 dt\frac{1}{t^3}\left\{\frac{t^2-1}{nt^2}P_{nl}(t)+\frac{2}{3n}-\frac{8}{3}t^2\delta_{l,0}\right\} - 2\ln(n)\delta_{l,0}. \quad (4)$$

The specification of the principal value is necessary in Eq. (4) because of bound-state poles whose residue gives the one-photon spontaneous decay width of an excited atomic state.

As an example, we consider here the $4P$ state for which the matrix element has the form

$$P_{n=4,l=1}(t) = -\frac{1024\,t^7}{45(t-1)^8(t+1)^8}\Phi(4,t)[75-1700\,t^2 + 9954\,t^4 - 21\,124\,t^6 + 14\,907\,t^8] + \frac{2t^2}{45(t-1)^8(t+1)^8}[15-30\,t-60\,t^2+150\,t^3 + 1547\,t^4 + 15\,956\,t^5 - 154\,368\,t^6 - 142\,420\,t^7 + 1\,166\,645\,t^8 + 357\,354\,t^9 - 2\,744\,516\,t^{10} - 276\,066\,t^{11} + 2\,046\,129\,t^{12}]. \quad (5)$$

The "standard hypergeometric" function which occurs in this expression, is encountered in various previous calculations[28,29]

$$\Phi(n,t) = {}_2F_1\left(1,-nt,1-nt,\left(\frac{1-t}{1+t}\right)^2\right) = -nt\sum_{k=0}^{\infty}\frac{\left(\frac{1-t}{1+t}\right)^{2k}}{k-nt}. \quad (6)$$

The convergence of this series representation near $t=0$ is problematic, but it can be accelerated effectively using the combined nonlinear-condensation transformation (CNCT) described in Refs. [31,32]. Using this method, we easily obtain the 40-figure result

$$\ln k_0(n=4,l=1) = -0.041\,954\,894\,598\,085\,548\,671\,037\,594\,335\,271\,341\,857\,0, \quad (7)$$

which is consistent with the 24-figure result given in Eq. (64) of Ref. [32] and with the 27-figure result given in Table III of Ref. [39] for this state.

The number of terms occurring in Eq. (5) is not excessive, but it grows rapidly with the angular momentum defect $\zeta = n-l$. In addition, considerable numerical cancellation can occur from the typically alternating sign pattern of the polynomial that multiplies $\Phi(n,t)$. For circular Rydberg states with $n=l+1$, the analytic expressions obtained for $P(t)$ are most compact, and these states can be well treated using the integral representation, up to very high principal quantum numbers.

We found that, using the integral representation, numerically satisfactory results can be obtained for states with $\zeta = n-l < 5$, in the entire range $n \leqslant 200$. However, for $\zeta = n-l > 5$, the accuracy obtained using this method was not satisfactory, unless an excessively accurate multiprecision arithmetic is used in intermediate steps of the calculation. It is still possible to use the integral representation for $n-l \leqslant 20$. In this case, one does not have more than 19 sbound-state poles to subtract in forming the principal value in Eq. (4). As an alternative, one may deform the t-integration contour into the complex plane. However, for $\zeta = n-l \leqslant 20$, we found the numerical difficulties to be so severe that a different method of calculation appeared to be called for. The more complex structure of the wave function with increasing $n-l$ is illustrated in Fig. 1.

However, before we resort to this different method, in Sec. III below, we briefly dwell on the application of the integral representation to circular states with $n=l+1$. It is possible to give a general integral representation for the Bethe logarithm of a circular state with $l=n-1, n>1$. This representation is a specialization of Eq. (4) and reads

$$\ln k_0(n,n-1) = -\frac{3}{4}\int_0^1 dt\, f(t). \quad (8)$$

Here,

$$f(t) = -\frac{1-t^2}{nt^5}\left[-\frac{2t^2}{3(1-t^2)} + \sum_{k=0}^{\infty} T(k,n,t)\right]. \quad (9)$$

The term $T(k,n,t)$ is given by

$$T(k,n,t) = -\frac{2^{4n}t^{2n}(1+t)^{-4n}}{(2n-1)\Gamma(2n)}\frac{1}{k!}\left(\frac{1-t}{1+t}\right)^{2k} \times\left[\frac{(n-1)t[\mathcal{P}(k,n,t)]^2\Gamma(k+2n-2)}{3n(1-t)^4(1-k-n+nt)} + \frac{4t^3\Gamma(k+2n+2)}{3(1+t)^4(-1-k-n+nt)}\right]. \quad (10)$$

The polynomial $\mathcal{P}(k,n,t)$ reads

$$\mathcal{P}(k,n,t) = (k+n-1)(2n-1)(1-t)^2 - 2tk(k-1). \quad (11)$$

The first term on the right-hand side of Eq. (10) has a singularity at $t=(n-1)/n$, which corresponds to the decay into the lower-lying state with principal quantum number $n-1$ and orbital angular momentum quantum number $l=n-2$. Selected numerical values for very highly excited hydrogenic states, obtained using the integral representation, are given in Table I.

TABLE I. Values of Rydberg state Bethe logarithms near $n \approx 100$, for small angular momentum defect $\zeta = n - l$. The results displayed here can be obtained using both the integral representation as well as the spectral representation of the Bethe logarithm, and both methods were used in order to check the consistency of the results.

$\ln k_0(n, n-\zeta)$	$\zeta=1$	$\zeta=2$	$\zeta=3$	$\zeta=4$
$n=100$	$-0.583\ 308\ 014\times10^{-7}$	$-0.613\ 877\ 681\times10^{-7}$	$-0.645\ 944\ 796\times10^{-7}$	$-0.679\ 594\ 629\times10^{-7}$
$n=101$	$-0.566\ 008\ 997\times10^{-7}$	$-0.595\ 371\ 896\times10^{-7}$	$-0.626\ 158\ 390\times10^{-7}$	$-0.658\ 448\ 703\times10^{-7}$
$n=102$	$-0.549\ 387\ 309\times10^{-7}$	$-0.577\ 602\ 405\times10^{-7}$	$-0.607\ 171\ 570\times10^{-7}$	$-0.638\ 170\ 329\times10^{-7}$
$n=103$	$-0.533\ 410\ 121\times10^{-7}$	$-0.560\ 532\ 956\times10^{-7}$	$-0.588\ 944\ 368\times10^{-7}$	$-0.618\ 715\ 502\times10^{-7}$
$n=104$	$-0.518\ 046\ 496\times10^{-7}$	$-0.544\ 129\ 416\times10^{-7}$	$-0.571\ 439\ 188\times10^{-7}$	$-0.600\ 042\ 866\times10^{-7}$
$n=105$	$-0.503\ 267\ 262\times10^{-7}$	$-0.528\ 359\ 632\times10^{-7}$	$-0.554\ 620\ 643\times10^{-7}$	$-0.582\ 113\ 531\times10^{-7}$
$n=106$	$-0.489\ 044\ 896\times10^{-7}$	$-0.513\ 193\ 296\times10^{-7}$	$-0.538\ 455\ 408\times10^{-7}$	$-0.564\ 890\ 904\times10^{-7}$
$n=107$	$-0.475\ 353\ 416\times10^{-7}$	$-0.498\ 601\ 821\times10^{-7}$	$-0.522\ 912\ 079\times10^{-7}$	$-0.548\ 340\ 528\times10^{-7}$
$n=108$	$-0.462\ 168\ 279\times10^{-7}$	$-0.484\ 558\ 230\times10^{-7}$	$-0.507\ 961\ 045\times10^{-7}$	$-0.532\ 429\ 945\times10^{-7}$
$n=109$	$-0.449\ 466\ 295\times10^{-7}$	$-0.471\ 037\ 051\times10^{-7}$	$-0.493\ 574\ 371\times10^{-7}$	$-0.517\ 128\ 556\times10^{-7}$
$n=110$	$-0.437\ 225\ 533\times10^{-7}$	$-0.458\ 014\ \ 220\times10^{-7}$	$-0.479\ 725\ 687\times10^{-7}$	$-0.502\ 407\ 501\times10^{-7}$

III. SPECTRAL REPRESENTATION

The integral representation discussed in Sec. II very closely reflects the physics involved in the original problem, by expressing the Bethe logarithm as an integral over the energy of a virtual photon. For computational purposes, a different method can be more effective, which relies on available analytic results for transition matrix elements of discrete-discrete transitions [40], as cited in Eq. (63.2) of Ref. [41], and for discrete-continuum transitions see Eq. (6) of Ref. [42] or alternatively Ref. [43]. Note that in Eq. (6) of Ref. [42], the argument of the arccot function in the exponential should be replaced according to $n'n/n \to n'/n$, and that, as pointed out in Ref. [44], the continuum wave functions used in Ref. [42] are normalized to the energy scale, not to the momentum scale. The latter fact implies that Eq. (3b) of Ref. [42] receives a correction according to Eq. (3b) of Ref. [44]. For the transition matrix elements of selected low-lying states into the continuum, one may alternatively use the formulas given in Ref. [45], but one should be aware of multiplicative correction factors as pointed out below Eq. (11) of Ref. [17].

The spectral representation is based on the following formula for the Bethe logarithm,

$$\ln k_0(n,l) = \frac{n^3}{2(Z\alpha)^4 m} \left\langle \phi \left| \frac{p^i}{m} (H_S - E_n) \times \ln\left[\frac{2|H_S - E_n|}{(Z\alpha)^2 m} \right] \frac{p^i}{m} \right| \phi \right\rangle, \tag{12}$$

where $|\phi\rangle = |nlm\rangle$. Here, H_S is the Schrödinger Hamiltonian

$$H_S = \frac{p^2}{2m} - \frac{Z\alpha}{r}. \tag{13}$$

This spectrum of this operator, as is well known, has a discrete part (bound states, $E_n < 0$), and a continuous part (continuum states, $E > 0$). Note that the modulus $|H_S - E_n|$ is involved in Eq. (12). Otherwise, the argument of the logarithm could become negative. The specification of the modulus corresponds to the principal value prescription in Eq. (4). Using the commutator relation $p^i = \mathrm{i}\, m[H_S, r^i]$, one may easily transform Eq. (12) into

$$\ln k_0(n,l) = \frac{n^3}{2(Z\alpha)^4 m} \left\langle \phi \left| r^i (H_S - E_n)^3 \ln\left[\frac{2|H_S - E_n|}{(Z\alpha)^2 m} \right] r^i \right| \phi \right\rangle. \tag{14}$$

We assume the wave functions of the continuous spectrum to be normalized according to

$$\langle Elm | E' l' m' \rangle = \delta(E - E')\, \delta_{ll'} \delta_{mm'}. \tag{15}$$

The discrete spectrum is normalized according to $\langle nlm | n' l' m' \rangle = \delta_{nn'} \delta_{ll'} \delta_{mm'}$. One may then write down a spectral decomposition of Eq. (12),

$$\begin{aligned} \ln k_0(n,l) &= \frac{n^3}{2(Z\alpha)^4 m} \sum_{i=1}^{3} \left\langle nlm \left| r^i (H_S - E_n)^3 \times \ln\left[\frac{2|H_S - E_n|}{(Z\alpha)^2 m} \right] r^i \right| nlm \right\rangle \\ &= \frac{n^3}{2(Z\alpha)^4 m} \sum_{n'=0}^{\infty} \sum_{l'=l\pm1} \sum_{m'=-l'}^{l'} \sum_{i=1}^{3} (E_{n'} - E_n)^3 \times \ln\left[\frac{2|E_{n'} - E_n|}{(Z\alpha)^2 m} \right] |\langle nlm | r^i | n' l' m' \rangle|^2 \\ &\quad + \frac{n^3}{2(Z\alpha)^4 m} \int_0^{\infty} \mathrm{d}E' \sum_{l'=l\pm1} \sum_{m'=-l'}^{l'} \sum_{i=1}^{3} (E' - E_n)^3 \times \ln\left[\frac{2|E' - E_n|}{(Z\alpha)^2 m} \right] |\langle nlm | r^i | E' l' m' \rangle|^2 = B + C. \end{aligned} \tag{16}$$

Here, B is the bound-spectrum contribution, and C stems from the continuum. Using the dipole selection rules, one immediately sees that the angular sums over l' collapse to only two nonvanishing terms. We assume the wave functions

TABLE II. Sample values of Rydberg state Bethe logarithms near $n \approx 200, 0 \leqslant l \leqslant 3$. All decimal figures shown are significant. The values are consistent with a constant limit for $\ln k_0(n,l)$ as $n \to \infty$ for constant l. In contrast to Table I, the values displayed here have been obtained exclusively using the spectral representation. Note that the entries are labeled as $\ln k_0(n,l)$ in contrast to the notation $\ln k_0(n, n-\zeta)$ used in Table I.

$\ln k_0(n,l)$	$l=0$	$l=1$	$l=2$	$l=3$
$n=190$	$0.272\ 266\ 958 \times 10^{1}$	$-0.490\ 489\ 444 \times 10^{-1}$	$-0.993\ 712\ 588 \times 10^{-2}$	$-0.355\ 864\ 236 \times 10^{-2}$
$n=191$	$0.272\ 266\ 942 \times 10^{1}$	$-0.490\ 490\ 025 \times 10^{-1}$	$-0.993\ 716\ 023 \times 10^{-2}$	$-0.355\ 866\ 654 \times 10^{-2}$
$n=192$	$0.272\ 266\ 927 \times 10^{1}$	$-0.490\ 490\ 596 \times 10^{-1}$	$-0.993\ 719\ 406 \times 10^{-2}$	$-0.355\ 869\ 035 \times 10^{-2}$
$n=193$	$0.272\ 266\ 911 \times 10^{1}$	$-0.490\ 491\ 159 \times 10^{-1}$	$-0.993\ 722\ 737 \times 10^{-2}$	$-0.355\ 871\ 380 \times 10^{-2}$
$n=194$	$0.272\ 266\ 896 \times 10^{1}$	$-0.490\ 491\ 713 \times 10^{-1}$	$-0.993\ 726\ 017 \times 10^{-2}$	$-0.355\ 873\ 690 \times 10^{-2}$
$n=195$	$0.272\ 266\ 881 \times 10^{1}$	$-0.490\ 492\ 258 \times 10^{-1}$	$-0.993\ 729\ 247 \times 10^{-2}$	$-0.355\ 875\ 964 \times 10^{-2}$
$n=196$	$0.272\ 266\ 867 \times 10^{1}$	$-0.490\ 492\ 796 \times 10^{-1}$	$-0.993\ 732\ 428 \times 10^{-2}$	$-0.355\ 878\ 205 \times 10^{-2}$
$n=197$	$0.272\ 266\ 852 \times 10^{1}$	$-0.490\ 493\ 325 \times 10^{-1}$	$-0.993\ 735\ 562 \times 10^{-2}$	$-0.355\ 880\ 412 \times 10^{-2}$
$n=198$	$0.272\ 266\ 838 \times 10^{1}$	$-0.490\ 493\ 846 \times 10^{-1}$	$-0.993\ 738\ 649 \times 10^{-2}$	$-0.355\ 882\ 586 \times 10^{-2}$
$n=199$	$0.272\ 266\ 824 \times 10^{1}$	$-0.490\ 494\ 360 \times 10^{-1}$	$-0.993\ 741\ 690 \times 10^{-2}$	$-0.355\ 884\ 728 \times 10^{-2}$
$n=200$	$0.272\ 266\ 810 \times 10^{1}$	$-0.490\ 494\ 865 \times 10^{-1}$	$-0.993\ 744\ 687 \times 10^{-2}$	$-0.355\ 886\ 838 \times 10^{-2}$

to have the structure $\langle r|nlm\rangle = R_{nl}(r) Y_{lm}(\theta,\phi)$ and $\langle r|Elm\rangle = \mathcal{R}_{El}(r) Y_{lm}(\theta,\phi)$, where θ and ϕ are the polar angles. In terms of radial integrals, the quantities B and C read

$$B = \frac{n^3}{2(Z\alpha)^4 m}\left\{ \frac{l}{2l+1} \sum_{n'=0}^{\infty} (E_{n'} - E_n)^3 \ln\left[\frac{2|E_{n'} - E_n|}{(Z\alpha)^2 m}\right] \times \left| \int_0^\infty \mathrm{d}r\, r^3 R_{nl}(r) R_{n'(l-1)}(r) \right|^2 + \frac{l+1}{2l+1} \sum_{n'=0}^{\infty} (E_{n'} - E_n)^3 \times \ln\left[\frac{2|E_{n'} - E_n|}{(Z\alpha)^2 m}\right] \left| \int_0^\infty \mathrm{d}r\, r^3 R_{nl}(r) R_{n'(l+1)}(r) \right|^2 \right\} \tag{17a}$$

and

$$C = \frac{n^3}{2(Z\alpha)^4 m}\left\{ \frac{l}{2l+1} \int_0^\infty \mathrm{d}E' (E' - E_n)^3 \ln\left[\frac{2|E' - E_n|}{(Z\alpha)^2 m}\right] \times \left| \int_0^\infty \mathrm{d}r\, r^3 R_{nl}(r) \mathcal{R}_{E'(l-1)}(r) \right|^2 + \frac{l+1}{2l+1} \int_0^\infty \mathrm{d}E' (E' - E_n)^3 \times \ln\left[\frac{2|E' - E_n|}{(Z\alpha)^2 m}\right] \left| \int_0^\infty \mathrm{d}r\, r^3 R_{nl}(r) \mathcal{R}_{E'(l+1)}(r) \right|^2 \right\}. \tag{17b}$$

The representations (17a) and (17b) involve only radial integrals; therefore Eq. (63.2) of Ref. [41] and Eq. (6) of Ref. [42] can be directly applied (with the above mentioned correction in the argument of the arccot function). In the calculation of B, the CNCT [31,32] was used in order to accelerate the convergence of the sum over n'. For the evaluation of C, a simple Gaussian integration was found to be appropriate after a suitable variable change that maps the interval $E' \in (0,\infty)$ onto the compact interval (0, 1).

Selected numerical in values for very highly excited Rydberg states with principal quantum numbers $n \leqslant 200$, obtained using the spectral representation, can be found in Tables II–IV. The values listed in Table II are consistent with the asymptotic expansions in Appendix B, as given in Eqs. (B2) and (B3), and in Table V (see also Refs. [45,46]). For circular states, the values given in Table IV confirm the asymptotic expansion in Eq. (B1). Final numerical calculations were done using the high-performance computing facilities of the Max Planck Institute for Nuclear Physics in Heidelberg, and using a cluster of IBM Thinkpad mobile workstations [47]. Advantage has been taken of multiprecision libraries [48–51].

IV. CONCLUSIONS

We have presented the evaluation of Bethe logarithms for all the 20,100 hydrogenic states with a principal quantum number $n \leqslant 200$. Two methods have been used: The first method involves an integral representation which reflects the physics of the underlying phenomenon in a very direct manner, by expressing the Bethe logarithm in terms of an integral over the virtual photon energy (see Sec. II). The second method relies on a spectral decomposition of the Bethe logarithm (see Sec. III). In that latter representation, the two distinct contributions from virtual discrete states and virtual bound states can be clearly distinguished. A third method, which has been used in exploratory work, is briefly described in Appendix A. Selected numerical data are presented in Eq. (7) and in the Tables I–IV. The full set of numerical values is available in [52].

Incidentally, we observe that for all states which simultaneously fulfill $150 \leqslant n \leqslant 200$ and $l \geqslant 150$, the virtual bound states give by far the dominant contribution to the Bethe logarithm; indeed, we have $|B/C| > 10^{10}$ for these states [for the definition of B and C see Eqs. (17a) and (17b)]. This

TABLE III. Values of Rydberg state Bethe logarithms near $n \approx 200, 100 \leqslant l \leqslant 103$. This table complements Table I, by investigating a range of quantum numbers where both the principal quantum number n as well as the orbital angular momentum quantum number l are large. The angular momentum defect $\xi = n - l$ is also large for all states in this table. As for the entries in Table II, the values are consistent with a constant limit as $n \to \infty$ for given l.

$\ln k_0(n,l)$	$l=100$	$l=101$	$l=102$	$l=103$
$n=190$	$-0.108\ 830\ 510 \times 10^{-6}$	$-0.105\ 112\ 540 \times 10^{-6}$	$-0.101\ 547\ 415 \times 10^{-6}$	$-0.981\ 275\ 887 \times 10^{-7}$
$n=191$	$-0.109\ 118\ 840 \times 10^{-6}$	$-0.105\ 395\ 841 \times 10^{-6}$	$-0.101\ 825\ 818 \times 10^{-6}$	$-0.984\ 012\ 208 \times 10^{-7}$
$n=192$	$-0.109\ 403\ 831 \times 10^{-6}$	$-0.105\ 675\ 864 \times 10^{-6}$	$-0.102\ 101\ 004 \times 10^{-6}$	$-0.986\ 716\ 920 \times 10^{-7}$
$n=193$	$-0.109\ 685\ 537 \times 10^{-6}$	$-0.105\ 952\ 663 \times 10^{-6}$	$-0.102\ 373\ 023 \times 10^{-6}$	$-0.989\ 390\ 540 \times 10^{-7}$
$n=194$	$-0.109\ 964\ 013 \times 10^{-6}$	$-0.106\ 226\ 290 \times 10^{-6}$	$-0.102\ 641\ 927 \times 10^{-6}$	$-0.992\ 033\ 569 \times 10^{-7}$
$n=195$	$-0.110\ 239\ 309 \times 10^{-6}$	$-0.106\ 496\ 796 \times 10^{-6}$	$-0.102\ 907\ 766 \times 10^{-6}$	$-0.994\ 646\ 499 \times 10^{-7}$
$n=196$	$-0.110\ 511\ 476 \times 10^{-6}$	$-0.106\ 764\ 231 \times 10^{-6}$	$-0.103\ 170\ 590 \times 10^{-6}$	$-0.997\ 229\ 814 \times 10^{-7}$
$n=197$	$-0.110\ 780\ 565 \times 10^{-6}$	$-0.107\ 028\ 643 \times 10^{-6}$	$-0.103\ 430\ 446 \times 10^{-6}$	$-0.999\ 783\ 983 \times 10^{-7}$
$n=198$	$-0.111\ 046\ 625 \times 10^{-6}$	$-0.107\ 290\ 080 \times 10^{-6}$	$-0.103\ 687\ 382 \times 10^{-6}$	$-0.100\ 230\ 947 \times 10^{-6}$
$n=199$	$-0.111\ 309\ 701 \times 10^{-6}$	$-0.107\ 548\ 591 \times 10^{-6}$	$-0.103\ 941\ 443 \times 10^{-6}$	$-0.100\ 480\ 673 \times 10^{-6}$
$n=200$	$-0.111\ 569\ 843 \times 10^{-6}$	$-0.107\ 804\ 219 \times 10^{-6}$	$-0.104\ 192\ 674 \times 10^{-6}$	$-0.100\ 727\ 619 \times 10^{-6}$

observation is in sharp contrast to lower-lying states, where $|B/C|$ is typically smaller than one. e.g., the ground state fulfills $|B/C| \approx 0.00483$. We conclude that the contribution of virtual bound states as compared to virtual continuum states is much more pronounced for Rydberg states as compared to lower-lying states, an observation which might appear counterintuitive at first glance.

ACKNOWLEDGMENTS

U.D.J. acknowledges helpful conversations with Professor Krzysztof Pachucki and support from the National Institute of Standards and Technology during a number of research appointments. Sabine Jentschura is acknowledged for carefully reading the manuscript, and for extensive help in the numerical calculations regarding the comparison of the results of the current investigation to those of Ref. [46]. We also thank an anonymous referee for some helpful remarks.

Appendix A: Lattice Schrödinger–Coulomb Propagator

The computational implementation of the Schrödinger propagator on a discrete lattice has been discussed in Ref. [36]. It can lead to a computationally cheap evaluation procedure, provided that the required numerical accuracy is not excessive. Numerical difficulties grow for higher excited states, in both one- and two-loop quantum electrodynamic problems, for of a number of reasons (more terms and in general a more complex structure of the wave function, more bound-state poles along the integration contours, more nodes of the wave function, which translate into numerical cancellations, etc.). While of course any computational method is expandable, we have found it difficult to control the accuracy of the Bethe logarithm, calculated using a discrete-lattice representation, for both for high n as well as for high $\zeta = n - l$. For high n, the wave function extends over many Bohr radii, which necessitates an accurate representation of the Schrödinger–Coulomb propagator over an extended grid, which is difficult to achieve with a limited grid size. For high ζ, the difficulties are enhanced due to the oscillations of the wave function which necessitate an even more accurate representation on the grid.

In exploring this way of calculating the Bethe logarithm, we found it instructive, however, to use routines which lead to an explicit diagonalization of the Schrödinger–Coulomb propagator on the grid. The accuracy of the lowest virtual-state energy eigenvalues is actually satisfactory, while for higher excited virtual states, the eigenvalues depart rapidly from the exact Schrödinger solution $E_n = -(Z\alpha)^2 m/(2n^2)$. This phenomenon has also been observed in the context of basis-set calculations of relativistic effects in atoms which rely on B-spline techniques, see e.g. Ref. [35]. On a discrete lattice, one can in principle only obtain a discrete spectrum, which for the Schrödinger–Coulomb propagator extends into

TABLE IV. Values of Rydberg state Bethe logarithms near $n \approx 200$, for the highest principal quantum numbers and angular momenta under investigation in this article. The angular momentum defect is small for the states listed in this table. Conse- quently, the states listed here can be calculated using both the integral as well as the spectral representation.

$\ln k_0(n,l)$	$l=196$	$l=197$	$l=198$	$l=199$
$n=197$	$-0.753\ 369\ 175 \times 10^{-8}$			
$n=198$	$-0.761\ 387\ 888 \times 10^{-8}$	$-0.741\ 963\ 223 \times 10^{-8}$		
$n=199$	$-0.769\ 316\ 490 \times 10^{-8}$	$-0.749\ 821\ 211 \times 10^{-8}$	$-0.730\ 786\ 360 \times 10^{-8}$	
$n=200$	$-0.777\ 156\ 469 \times 10^{-8}$	$-0.757\ 591\ 335 \times 10^{-8}$	$-0.738\ 487\ 630 \times 10^{-8}$	$-0.719\ 832\ 864 \times 10^{-8}$

TABLE V. Numerical values of the limits $\ln k_0(\infty,l) \equiv \lim_{n\to\infty} \ln k_0(n,l)$ for $l=0,\ldots,10$. The evaluation proceeds according to methods outlined in Ref. [46]; the values communicated here are in agreement with and more accurate than those obtained for the range $l=0, \ldots, 7$ in Ref. [46].

l	$\ln k_0(\infty,l)$
0	+2.722 654 335
1	−0.049 054 544
2	−0.009 940 457
3	−0.003 560 999
4	−0.001 663 771
5	−0.000 908 042
6	−0.000 548 999
7	−0.000 356 923
8	−0.000 244 981
9	−0.000 175 372
10	−0.000 129 830

the positive-energy domain. It is then possible to use the eigenvalues and eigenvectors directly in order to evaluate the Bethe logarithm [in the sense of the bound-state contribution in Eq. (17a)]. This statement remains true although the higher excited virtual states "energies" on the lattice depart very much from the true eigenvalues $E_n=-(Z\alpha)^2 m/(2n^2)$ obtained for a Hamiltonian acting on $L^2(\mathbb{R}^3)$.

Using the lattice representation, it is easily possible to obtain about 9 decimal figures for the $1S$ Bethe logarithm on a lattice which extends to 20 Bohr radii and which is comprised of only 200 nodes. However, we have found it difficult to substantially enhance the accuracy, for low-lying states, beyond 20 figures, even if quadruple precision is used in the linear algebra libraries. This level of accuracy is of course dwarfed by other available methods, for the concrete problem at hand [see Eq. (7)], and, therefore, the lattice representation has not been pursued any further in the current context of Bethe logarithms for Rydberg states. However, we re-emphasize here that the lattice representation can lead to a computationally very efficient evaluation of matrix elements of the hydrogenic propagator, a property which has become useful in the calculation of other quantum electrodynamic effects for lower-lying states with $n\leqslant 6$ [4,53].

The limitation experienced in the attainable numerical accuracy for lattice calculations finds an explanation in view of two obvious limitations of this method: The size of the box determines the minimum energy (longest wavelength) solution that can be represented, and the longest lattice spacing determines the maximum energy (shortest wavelength) solution. The highly oscillatory behaviour of the radial wave function for Rydberg states (see also Fig. 1), which corresponds to short-wavelength components, cannot be accurately represented on a numerical lattice; this property affords a natural explanation for the difficulties experienced with the lattice-based method in the context of the current calculation.

Appendix B: Asymptotics derived previously

Based on an extrapolation of the numerical data of Table I of Ref. [5] to higher principal quantum numbers, the following asymptotics for the Bethe logarithm of circular Rydberg states had been obtained:

$$l^3 \times \ln k_0(l+1,l) \simeq -0.056\,852\,81(3) + \frac{0.024\,820\,8(6)}{l} + \frac{0.038\,14(2)}{l^2} - \frac{0.1145(5)}{l^3} + \frac{0.166(3)}{l^4} - \frac{0.22(2)}{l^5}. \tag{B1}$$

Here, terms of order l^{-k} with $k\geqslant 6$ are neglected. For S states, the following asymptotics had been obtained on the basis of the numerical data listed in Ref. [6]:

$$\ln k_0(n,l=0) \simeq 2.722\,654\,34(5) + \frac{0.000\,000(5)}{n} + \frac{0.553\,60(5)}{n^2} - \frac{0.5993(5)}{n^3} + \frac{0.613(7)}{n^4} - \frac{0.60(5)}{n^5}. \tag{B2}$$

The corresponding expression for P states reads

$$\ln k_0(n,l=1) \simeq -0.0490\,545(1) + \frac{0.000\,000(5)}{n} + \frac{0.205\,30(15)}{n^2} - \frac{0.599(5)}{n^3} + \frac{1.45(10)}{n^4} - \frac{3(1)}{n^5}. \tag{B3}$$

In an apparently not very widely known paper [46], a method has been indicated for the evaluation of the Bethe logarithm in the limit of infinite principal quantum number $n=\infty$. This method relies on an asymptotic expansion of the radial integrals that enter into Eqs. (17a) and (17b), in the

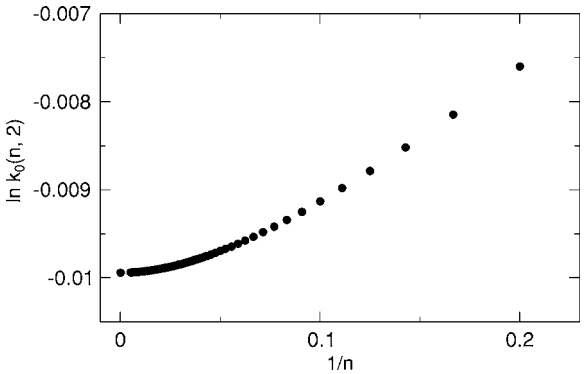

FIG. 2. The Bethe logarithms for $l=2$ (D states) are in excellent agreement with their asymptotic limit as $n\to\infty$. We plot here the values $\ln k_0(n,2)$ as a function of n^{-1}. For $n=190,\ldots,200$, the values of $\ln k_0(n,2)$ are given in Table II (see Ref. [52] for a complete list of all relevant values in the range $n\leqslant 200$). The limiting value at $n^{-1}=0$, which is $\ln k_0(\infty,2)=-0.994\,045\,690\times 10^{-2}$ (see also Table V), has been evaluated independently according to Ref. [46].

limit of an infinite principal quantum number of the reference state. The resulting integrals are very slowly convergent, but they permit a completely independent evaluation of $\ln k_0(\infty,l)$ which does not rely on an extrapolation of data available for lower principal quantum numbers [cf. Eqs. (B1)–(B3)]. Thus, the limiting values $\ln k_0(\infty,l)$ provide a sensitive independent crosscheck of the numerical methods employed in the current calculation.

In Ref. [46], the limits $\ln k_0(n=\infty,l)$ have been evaluated for $l=0,\ldots,7$. Here, we generalize the treatment to the range $l=0,\ldots,10$, thereby confirming the asymptotic limits obtained in Ref. [46] (see Table V). A comparison to the numerical values obtained in the current investigation indicates excellent agreement with the asymptotic values as $n\to\infty$ (see Fig. 2 for the case $l=2$). A full investigation of the asymptotic structure of Bethe logarithms for large n, including a derivation of the subleading terms in the expansion in powers of n^{-1}, would be very interesting in its own right. Such an investigation would be facilitated by the availability of accurate numerical data over wide ranges of n and l, as obtained in the current investigation.

[1] H. A. Bethe, Phys. Rev. **72**, 339 (1947).
[2] U. D. Jentschura, S. Kotochigova, E.-O. Le Bigot, P. J. Mohr, and B. N. Taylor, Phys. Rev. Lett. (to be published).
[3] U. D. Jentschura, J. Phys. A **36**, L229 (2003).
[4] U. D. Jentschura, Phys. Rev. A **70**, 052108 (2004).
[5] U. D. Jentschura, E.-O. Le Bigot, J. Evers, P. J. Mohr, and C. H. Keitel, J. Phys. B **38**, S97 (2005).
[6] G. W. F. Drake, and R. A. Swainson, Phys. Rev. A **41**, 1243 (1990).
[7] J. C. deVries, Ph.D. thesis, Massachusetts Institute of Technology, Cambridge, MA, 2002.
[8] A. Huber, T. Udem, B. Gross, J. Reichert, M. Kourogi, K. Pachucki, M. Weitz, and T. W. Hänsch, Phys. Rev. Lett. **80**, 468 (1998).
[9] J. L. Hall, L. S. Ma, M. Taubman, F. L. Hong, O. Pfister, and J. Ye, IEEE Trans. Instrum. Meas. **48**, 583 (1999).
[10] T. Udem, J. Reichert, R. Holzwarth, and T. W. Hänsch, Opt. Lett. **24**, 881 (1999).
[11] J. Reichert, M. Niering, R. Holzwarth, M. Weitz, T. Udem, and T. W. Hänsch, Phys. Rev. Lett. **84**, 3232 (2000).
[12] S. A. Diddams, D. J. Jones, J. Ye, S. T. Cundiff, J. L. Hall, J. K. Ranka, R. S. Windeler, R. Holzwarth, T. Udem, and T. W. Hänsch, Phys. Rev. Lett. **84**, 5102 (2000).
[13] D. J. Jones, S. A. Diddams, J. K. Ranka, A. Stentz, R. S. Windeler, J. L. Hall, and S. T. Cundiff, Science **288**, 635 (2000).
[14] J. Stenger, C. Tamm, N. Haverkamp, S. Weyers, and H. Telle, Opt. Lett. **26**, 1589 (2002).
[15] J. Stenger, H. Schnatz, C. Tamm, and H. R. Telle, Phys. Rev. Lett. **88**, 073601 (2002).
[16] P. J. Mohr, and B. N. Taylor, Rev. Mod. Phys. **77**, 1 (2005).
[17] H. A. Bethe, L. M. Brown, and J. R. Stehn, Phys. Rev. **77**, 370 (1950).
[18] J. M. Harriman, Phys. Rev. **101**, 594 (1956).
[19] C. Schwartz, and J. J. Tiemann, Ann. Phys. (N.Y.) **6**, 178 (1959).
[20] M. Lieber, Phys. Rev. **174**, 2037 (1968).
[21] R. W. Huff, Phys. Rev. **186**, 1367 (1969).
[22] S. Klarsfeld, and A. Maquet, Phys. Lett. B **43**, 201 (1973).
[23] I. Shimamura, J. Phys. Soc. Jpn. **40**, 239 (1976).
[24] S. E. Haywood, and J. D. Morgan, III, Phys. Rev. A **32**, 3179 (1985).
[25] J. T. Broad, Phys. Rev. A **31**, 1494 (1985).
[26] J. D. Baker, R. N. Hill, and J. D. Morgan, AIP Conf. Proc. **189**, 123 (1989).
[27] R. C. Forrey, and R. N. Hill, Ann. Phys. (N.Y.) **226**, 88 (1993).
[28] K. Pachucki, Ann. Phys. (N.Y.) **226**, 1 (1993).
[29] U. Jentschura, and K. Pachucki, Phys. Rev. A **54**, 1853 (1996).
[30] U. D. Jentschura, G. Soff, and P. J. Mohr, Phys. Rev. A **56**, 1739 (1997).
[31] U. D. Jentschura, P. J. Mohr, G. Soff, and E. J. Weniger, Comput. Phys. Commun. **116**, 28 (1999).
[32] S. V. Aksenov, M. A. Savageau, U. D. Jentschura, J. Becher, G. Soff, and P. J. Mohr, Comput. Phys. Commun. **150**, 1 (2003).
[33] V. I. Korobov, and S. V. Korobov, Phys. Rev. A **59**, 3394 (1999).
[34] G. W. F. Drake, and S. P. Goldman, Can. J. Phys. **77**, 835 (2000).
[35] W. R. Johnson, S. A. Blundell, and J. Sapirstein, Phys. Rev. A **37**, 307 (1988).
[36] S. Salomonson, and P. Öster, Phys. Rev. A **40**, 5559 (1989).
[37] W. Kuhn, and J. Strnad, *Quantenfeldtheorie* (Vieweg, Wiesbaden, Germany, 1995).
[38] U. D. Jentschura, and C. H. Keitel, Ann. Phys. (N.Y.) **310**, 1 (2004).
[39] S. P. Goldman, and G. W. F. Drake, Phys. Rev. A **61**, 052513 (2000).
[40] W. Gordon, Ann. Phys. **2**, 1031 (1929).
[41] H. A. Bethe, and E. E. Salpeter, *Quantum Mechanics of One and Two-Electron Atoms* (Springer, Berlin, 1957).
[42] N. Shafer and R. Bersohn, Phys. Rev. A **42**, 1313 (1990).
[43] W. J. Karzas, and R. Latter, Astrophys. J., Suppl. **6**, 167 (1961).
[44] N. Shafer, and R. Bersohn, Phys. Rev. A **44**, 7855 (1991).
[45] M. Stobbe, Ann. Phys. (Lpzg.) **7**, 661 (1930).
[46] A. Poquerusse, Phys. Lett. A **82**, 232 (1981).
[47] Certain commercial equipment, instruments, or materials are identified in this paper to foster understanding. Such identification does not imply recommendation or endorsement by the National Institute of Standards and Technology, nor does it imply that the materials or equipment identified are necessarily the best available for the purpose.
[48] S. Wolfram, *Mathematica—A System for Doing Mathematics*

by Computer (Addison-Wesley, Reading, MA, 1988).
[49] D. H. Bailey, NASA Ames Technical Report No. RNR-90-022.
[50] D. H. Bailey, ACM Trans. Math. Softw. **19**, 288 (1993).
[51] D. H. Bailey, NASA Ames Technical Report No. RNR-94-013. See also http://crd.lbl.gov/~dhbailey.
[52] See http://physics.nist.gov/hdel and http://www.mpi-hd.mpg.de/personalhomes/ulj. The full set of values is available at e-print quant-ph/0504002.
[53] K. Pachucki, and U. D. Jentschura, Phys. Rev. Lett. **91**, 113005 (2003).